Classification of Ultra-Wideband (UWB) Pulses Distorted by Penetration Effects

Thorsten Wehs, Allan C. Maheri, Carsten Koch

Hochschule Emden/Leer, University of Applied Sciences,

Department of Electronics and Informatics, Germany

Email: thorsten.wehs@hs-emden-leer.de, allan.christmas.maheri@uni-oldenburg.de, carsten.koch@hs-emden-leer.de

Abstract—One of the applications of Ultra-wideband pulses are in the area of indoor localization systems whereas the anchor nodes are placed at stationary positions on the ceiling or walls, while the mobile nodes can be located at any given location inside the building. The localization system has to estimate the location of the mobile nodes, but when the anchor nodes and the mobile nodes are separated by a solid material, such as a wall, wood, partition and glass, the performance of a localization system deteriorate due to distortion of UWB pulses as it penetrates the material. The quality of distortion is mainly affected by the type of material, thickness and the pulses' angle of incidence. In this paper, we analyse features which strongly characterizes the distorted pulses and with help of machine learning techniques, we present a framework for estimating the material type, material thickness and pulse's angle of incidence from a received distorted pulse. First, the material which distort the UWB pulse is classified, second the material thickness is assigned to four given classes of thickness and finally the pulse's angle of incidence is estimated.

I. Introduction

Ultra-Wideband(UWB) pulse technology has been applied in different fields of research and industry [1]. In most indoor applications, the technology provides a promising future for improving performance of real-time locating systems (RTLS) due to its ability of retaining the robustness of the signal under harsh environments such as in non-line-of-sight (NLOS) situations [2].

Nowadays, many indoor RTLS are equipped with UWB technology but there are still potential challenges which limit the performance of these systems. Some of these challenges include poor estimation of the location due to ranging errors which are caused by the penetration of walls, for instance in office buildings or hospitals. Such an indoor localization scenario is illustrated in Figure 1. In [3] and [4] the authors discussed the distortion of UWB pulses and the challenge of pulse detection for receiver algorithms. The NLOS effect *penetration of wall* might cause a huge bias which could be mitigated with the knowledge of the specific parameters of the penetrated wall, where the main parameters are the type of material (inherently permittivity and permeability), the thickness of the wall and the angle of incidence of the UWB pulse. If this information of the pulse path is known, the actual measured pulse travel time (ToF, time-of-flight) can be revised which results at least in an increased localization accuracy.

Regarding the scenario as shown in Figure 1, to range between a mobile target and e. g. anchor b means to pass a $10\,\mathrm{cm}$ wall of partition, which causes a bias of coarsely additional $10\,\mathrm{cm}$ each (assuming ToF ranging) which results in a significant localization error depending on the accuracy of the other rangings. By using standard multilateraton as described in [5], fact is the more accurate the input range values are, the more precisely the output localization solution is. If the bias of the measured ToF respectively ranges would be known, as addressed in this work, the localization accuracy could be significantly improved.
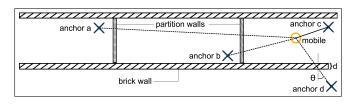

Fig. 1: Exemplary and schematic view on an indoor localization scenario e. g. in an office environment. The range measurements undergo penetration effects due to the walls within the buildung.

Due to the standardization process in building construction, there are typically a few different material types for walls. In addition, the bricks for walls have a few different standard thicknesses, varying from country to country. This results in standardized walls and the proposed approach is to classify this walls with a cascaded classification process. The parameters of the penetrated wall are derived from the characteristical distortion of the UWB pulse.

A. Motivation

The aim of the paper is to present an approach for classifying UWB pulses distorted by penetration effects. The main goal is to analyse features of a distorted UWB pulse, as well as to propose a framework that we use to estimate the angle of incidence and material thickness. However, compared to other approaches for estimating angle of incidence and material thickness which requires a theoretical model of the channel transmission or a full waveform of a received signal, our approach is mainly based on the analysis and characterization of the individual distorted UWB pulse.

B. Related work

Most localization algorithms are not robust in NLOS situations due to the increase in ranging errors. In NLOS situations, IR-UWB waveform undergoes distortion which resulted in poor estimation of location (i. e. when using ToF based ranging algorithms), because the ranging error is influenced by the distortion of the UWB pulse [6]. Therefore, techniques that can reduce ranging errors due to NLOS are called for. In the literature, this problem is divided into two sub problems: the first sub-problem is the *identification* of NLOS situations and the other sub-problem is the *mitigation* of the bias that is introduced due to NLOS [7]. In this paper we will focus on the latter sub-problem. Schroeder et al. presented in [8] a technique for NLOS identification and an improved detection technique of a distorted UWB pulse is covered in [3]. Now, the characterization of a distorted UWB pulse is required in order to improve the estimation of angle of incidence, material and wall thickness.

This paper consists of four sections. First section deduce our motivation and introduce the problem that we are addressing. The solution to the problem is presented in Section II, and the experimental set-up, evaluation and discussion of the results can be found in Section III. Section IV concludes the major outcome of this paper.

II. SOLUTION

In this section we present the basics of our approach: First, the estimation of the penetrated material, thickness and angle of incidence: The algorithm framework and the features that are utilized by a machine learning algorithm (i. e. we use a single layer artificial neural network) for classification. And the second step is the mitigation of the error influenced ToF values.

A. Classification framework

The framework consist of a five stage process as shown in Figure 2, and each stage can be described as follows:

1. *Distorted pulse*

   In the first stage, an UWB pulse distorted by penetration effects is detected and sampled (e. g. with leading edge detection as detailed by Haneda et al. in [9], Kuhn et al. in [10] or in [4]).

2. *Feature extraction*

   In the second stage, eight features of the detected distorted UWB pulse are extracted. These features include mean energy $\mu_{\mathbf{x}}$, amplitude ratio γ_{AMP}, kurtosis $\kappa_{\mathbf{x}}$, mean excess delay τ_{MED}, rms delay spread τ_{RMS}, area ratio γ_{AR}, symmetry ratio γ_{SYM} and skewness $\lambda_{\mathbf{x}}$.

3. *Material classification*

   In the third stage, the material which distort the UWB pulse is classified using a machine learning (ML) algorithm. The input are the extracted features of stage two which have been used to train the ML algorithm to recognize the patterns of the UWB pulses that are distorted by a specific material. In practice after the

training phase we would obtain $\binom{N}{2}$ decision boundaries, whereby N is the total number of material types.

4. *Thickness classification*

   In the fourth stage, penetrated material thickness classification is performed by training a second ML algorithm to recognize the patterns of the UWB pulses which are distorted by a standard known thickness of a particular material. Hence, after the training phase we would have $\binom{M}{2}$ decision boundaries, in which M is the total number of chosen thicknesses that are considered.

5. *Angle prediction*

   In the fifth and last stage, the prediction of the angle of incidence is performed. We observed in the analysed features that the RMS delay spread of a UWB pulse is proportional to the angle of incidence in various distortion conditions and differs for each material. An example of this relationship is illustrated in Figure 3. Hence, measuring the RMS delay spread, the angle of incidence can be predicted.

TABLE I
FEATURES WHICH ARE EXTRACTED FROM EACH DISTORTED PULSE.

No.	Features	Mathematical Formulation
1	Mean energy	$\mu_{\mathbf{x}} = \dfrac{1}{N}\sum\limits_{n=0}^{N}\mathbf{x}[n]$
2	Kurtosis	$\kappa_{\mathbf{x}} = \dfrac{1}{N}\sum\limits_{n=0}^{N}\left(\dfrac{\mathbf{x}[n]-\mu_{\mathbf{x}}}{\sigma_{\mathbf{x}}}\right)^4$
3	Mean excess delay	$\tau_{\mathrm{MED}} = \sum\limits_{n=0}^{N}\mathbf{x}[n]\left(\dfrac{|\mathbf{x}[n]|^2-\mu_{\mathbf{x}}}{\mathbf{x}^T\mathbf{x}}\right)$
4	RMS delay spread	$\tau_{\mathrm{RMS}} = \sum\limits_{n=0}^{N}(\mathbf{x}[n]-\tau_{\mathrm{MED}})^2\left(\dfrac{|\mathbf{x}[n]|^2}{\mathbf{x}^T\mathbf{x}}\right)$
5	Amplitude ratio	$\gamma_{\mathrm{AMP}} = \dfrac{|\max(\mathbf{x})|}{|\min(\mathbf{x})|}$
6	Area ratio	$\gamma_{\mathrm{AR}} = \dfrac{\sum\limits_{k=0}^{K}\mathbf{x}_+[k]}{\sum\limits_{m=0}^{M}\mathbf{x}_-[m]}$
7	Symmetry ratio	$\gamma_{\mathrm{SYM}} = \dfrac{\sum\limits_{n=0}^{\tau_{\mathrm{max}}}\mathbf{x}[n]^2}{\sum\limits_{n=\tau_{\mathrm{max}}+1}^{N}\mathbf{x}[n]^2}$
8	Skewness	$\lambda_{\mathbf{x}} = \dfrac{1}{N}\sum\limits_{n=0}^{N}\left(\dfrac{\mathbf{x}[n]-\mu_{\mathbf{x}}}{\sigma_{\mathbf{x}}}\right)^3$

The features which are extracted in step two and their respective mathematical formulation in discrete notation are detailed in Table IV, whereas $\mathbf{x}$ denotes a column vector which contains samples of a distorted UWB pulse, $\mathbf{x}_-$ and $\mathbf{x}_+$ denotes the negative and positive samples of $\mathbf{x}$ respectively, τ_{max} is the index of a sample which has maximum value in $\mathbf{x}$ and $\sigma_{\mathbf{x}}$ denotes the standard deviation of $\mathbf{x}$.

While the features 1 to 4 were taken from Marano et al. in [11], where they were used to perform a general LOS/NLOS
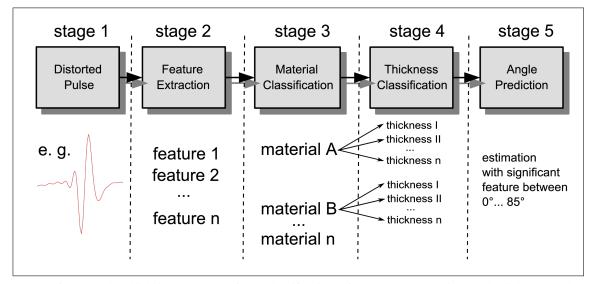
Fig. 2: Proposed framework which is used to perform classification of penetrated material, wall thickness and prediction of angle of incidence.

distinction, the feature 5 to 8 were developed by the authors to address especially the distorted shape of the pulse and his sidelobes.

B. Bias mitigation

Bias mitigation is the last step before localization estimation. Due to the lower velocity of signal propagation inside the wall, there is a bias in ToF. With the determined wall parameters from Section II-A the penetrated path through the wall $d_{pen.path}$ is calculated as follows:

$$d_{pen.path} = d_{wall} \cdot \frac{1}{\sqrt{1 - \sin^2\left(\frac{\theta}{\epsilon_r \cdot \mu_r}\right)}} \qquad (1)$$

Where d_{wall} is the thickness of the wall, θ the angle of incidence, ϵ_r the permittivity and μ_r the permeability the classified material of the wall. The measured ToF τ_{ToF} is now mitigated by the bias component τ_{bias}:

$$\begin{aligned} \tau_{true} &= \tau_{ToF} - \tau_{bias} \\ &= \tau_{ToF} - \frac{d_{pen.path}}{c_0 \left(\frac{1}{\sqrt{\epsilon_r \cdot \mu_r}} - 1\right)} \end{aligned} \qquad (2)$$

This results in the mitigated ToF τ_{true} which is multiplied by the speed of light c_0[1] equivalent to the bias-compensated spatial distance r between two radio transceivers:

$$r = \tau_{true} \cdot c_0 \qquad (3)$$

[1]We assume that the difference of speed of light between vacuum and air do not affect our results.

III. EXPERIMENTS AND PERFORMANCE

Simulations are carried out to evaluate the proposed framework based on synthetic distorted pulses which are generated according to the channel transmission model which was presented by Jing et al. in [12]. Three classes of materials (partition, drywall, brick) were used and the parameters for angle of incidence have been varied between $0°$ and $85°$ whereas the thickness of the material was fixed to four specific thicknesses (11.5 cm, 23 cm, 17.5 cm, 35 cm). Furthermore, 8 features which are described in Section II are extracted from each distorted UWB pulse and trained by an artificial neural network using MATLAB's Neural Network Toolbox.

Common classification using a supervised ML algorithm involve three steps which are training, cross validation and testing. In the training step the model which describes the data set is learned, the cross validation is aimed to choose the better learned model, and the testing step is to evaluate the performance of the learned model. Note that the default settings of the neural network from this toolbox have been employed for all simulations which randomly splits 70% of the original data set into training data, 15% for cross-validation and 15% for testing.

First, we create a database of synthetically distorted UWB pulses which comprises two types of data sets: The first data set (type I) is generated by varying the angle of incidence from $0°$ to $85°$ in steps of $0.5°$, while the second data set (type II) is generated by varying the angle of incidence from $0°$ to $85°$ with step of $1.48°$. The type II data set is used to do an additional performance evaluation of the 'optimal' neural network model which is obtained based on type I data set.

The generation of both datasets is done for each material and thickness meaning that the database contains a total number of 2748 distorted UWB pulses, out of which 2052 of distorted UWB pulses belongs to type I data set and 696 of the distorted UWB pulse belongs to type II dataset. A single layer artificial

neural network (**ANN**) architecture which has a total number of 18 neurons is used (quantity of neurons based on empirical experience).

Second, the classification of material and thickness is performed. The prediction of angle of incidence is done as described in Section II. Technically speaking, the type I data set were plugged into the ANN and since the material type, thickness and angle of incidence which distorted the UWB pulse is known, these are labelled data and the task of ANN is to learn the hidden models (of specific material type, and thickness) which distort the pulses. The type I data set is then split into training set, cross validation set and testing set according to the default settings of MATLAB.

The performance of ANN classification based on type I data set can either be measured using a confusion matrix, the receiver operating characteristics (**ROC**), or the behaviour of the cross entropy. We use the behaviour of cross entropy to describe the performance of ANN classifiers, because of the resulting verifiable quality parameters. In brief, cross entropy is the error function that is minimized by the algorithm which is used to train a neural network. Theoretical and experimental comparison between cross entropy and sum of square error in ANN related algorithms can be found in [13] where the authors found out that, training with cross entropy function, minimizes classification errors. Figure 4 and 5 show the plots of cross entropy in both classification of material and classification of thickness respectively using type I data set. The cross entropy in both cases is decreasing and has low values, which indicates a reliable classification result. In extreme cases when cross entropy is zero, that means there is no error in classification.
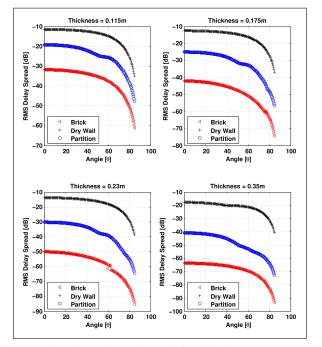
The real performance of the framework is evaluated at each stage separately using the type II data set. However, we are interested in the performance of learned neural network models on this data set, where we measure (percent correct) how well the ANN would be in recognizing material type and thickness which is shown in Table II and Table III. The results indicates the performance in all classification task is above 90%, and the UWB pulses which are distorted by a brick wall can be easily identified compared to other materials.
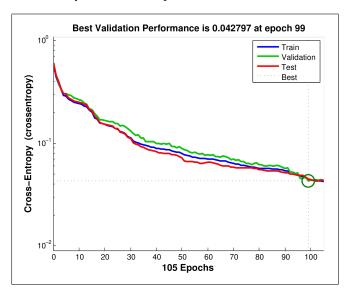

Fig. 4: The performance of trained neural network with first type data set which is used to classify penetrated material.

Fig. 3: The plots shows the relationship between root mean square delay spread τ_{RMS} and angle of incidence θ. This relationship is useful in the prediction of the angle of incidence.
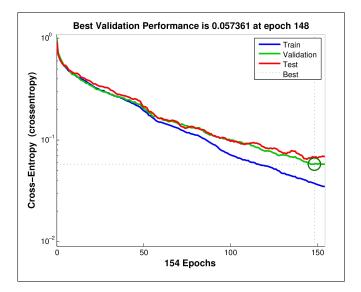

Fig. 5: The performance of trained neural network with first type data set which is used to classify penetrated material thickness.

The performance of angle prediction is presented in Figure 6 by the plots of the squares of the prediction error as a function of angle. However, the causes of included outlier are not yet

discussed in this paper and subject of further work. The pulse index is in context the serial number of the pulses in data set type II.

Material type	Performance on type II data set (%)
Partition	94.40
Dry Wall	98.71
Brick	99.14

Thickness (cm)	Performance on type II data set(%)
11.5	98.28
17.5	92.57
23.0	96.55
35.0	98.85

Regarding the problem as addressed in Section I, that means that in over 90% for every penetration case the parameters, which are crucial for the size of the bias due to through-wall propagation, can be classified correctly. With these parameters and the equations from Section II-B the mitigated time-of-flight and thereby the more accurate spatial distance could be determined. However, the fifth stage of our framework, the angle prediction, has an inherent risk of bigger prediction errors due to the dependence on only one feature. If this feature has a lower grade, i. e. in real world environments, the accuracy of the predicted angles of incidence would be decreased. So, in Table IV are presented some exemplifying good- and bad-case scenarios for the following penetration case: brick ($\bar{\epsilon}_r \approx 4.43$, $\mu_r \approx 1$), $d_{wall} = 23.0\,\mathrm{cm}$ and $\theta_{true} = 10°$ (Equations cp. Section II-B; assumption is that classification of material type and wall thickness was correct).

$\Delta_\theta/°$	$\theta_{pred}/°$	$d_{pen.path}/$cm	$r_{bias}/$cm	$\Delta_r/$cm
0	10	23.0	25.4	0.0
10	20	23.1	25.5	-0.1
30	40	23.3	25.7	-0.3
70	80	24.2	26.7	-1.3

Δ_θ is the error of the predicted angle θ_{pred} and Δ_r is the remaining error after the bias mitigation with error afflicted angle predictions. So, for this scenario there is only a small error due to a weak performance in the stage angle prediction. In column r_{bias} is listed the overall bias of the range, calculated with the wall parameters which were determined by the framework. This bias is mitigated in Equation 2.

IV. CONCLUSION

The aim of this work was to analyse features which retains more information of distorted UWB pulses and to present an approach which could be useful in prediction of angle of incidence, material type and wall thickness as amongst the crucial
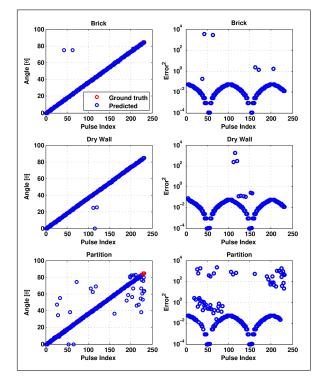

Fig. 6: Comparison between the estimated angle of incidence and its true value, also on the lower panel is the square prediction error which show in most cases the prediction error is lower but higher where prediction fails.

parameters of RTLS in localization of the mobile nodes. Our results show that the analysed features and the approach which is used, can guarantee significant performance. The experiment shows that for every parameter combination a hit rate of over 90% is achieved.

However, in this paper the data resource is completely synthetic because of the huge spectrum of wall parameters and measurement scenarios. So, to verify the shown results with real world data an extensive measurement campaign is necessary. Until then an improvement of the current experiment is to use synthetic data, which is combined with a standardized channel model for UWB propagation in indoor environments to get more realistic waveforms. A further point is the analysis of the computational cost of the proposed approach, which is necessary to know for productive use.

REFERENCES

[1] H. Wymeersch, S. Marano, W. M. Gifford, and M. Z. Win, "A Machine Learning Approach to Ranging Error Mitigation for UWB Localization," *IEEE Transactions on Communications*, vol. 60, no. 6, pp. 1719–1728, 2012.

[2] C. Chen, D. Hong, H. Xiaotao, L. Xiangyang, and Y. Jibing, "Through-wall localization with UWB sensor network," in *Ultra-Wideband (ICUWB), 2012 IEEE International Conference on*, 2012, pp. 284–287.

[3] T. Wehs, T. Leune, G. v. Cölln, and C. Koch, "Detection of distorted IR-UWB pulses in low SNR NLOS scenarios," *IEEE International Conference on Ultra-WideBand (ICUWB), Paris*, 2014.

[4] T. Wehs, T. Leune, C. Koch, and G. v. Cölln, "Improved Detection of Distorted IR-UWB Pulses Using Amplitude Spectrum in Indoor Environments," *IEEE International Conference on Indoor Positioning and Indoor Navigation 2014 (IPIN), Busan (Korea)*, 2014.

[5] T. Leune, T. Wehs, M. Janssen, C. Koch, and G. v. Colln, "Optimization of wireless locating in complex environments by placement of anchor nodes with evolutionary algorithms," in *Emerging Technologies & Factory Automation (ETFA), 2013 IEEE 18th Conference on*, 2013, pp. 1–6.

[6] J. Meng, Q.-Y. Zhang, and N. tong Zhang, "Impact of IR-UWB waveform distortion on NLOS localization system," in *Ultra-Wideband, 2009. ICUWB 2009. IEEE International Conference on*, Sept 2009, pp. 123–128.

[7] Stefano Marano, Wesley M. Gifford, Henk A.H.E Wymeersch, and Moe Z. Win, "Method and system for identification and mitigation of errors in non-line-of-sight distance estimation," Patent US 2011/0 177 786 A1, 2011.

[8] J. Schroeder, S. Galler, K. Kyamakya, and K. Jobmann, "NLOS detection algorithms for ultra-wideband localization," in *Positioning, Navigation and Communication, 2007. WPNC '07. 4th Workshop on*, March 2007, pp. 159–166.

[9] K. Haneda, K. i. Takizawa, J. i. Takada, M. Dashti, and P. Vainikainen, "Performance evaluation of threshold-based UWB ranging methods - Leading edge vs. search back -," in *Antennas and Propagation, 2009. EuCAP 2009. 3rd European Conference on*, 2009, pp. 3673–3677. [Online]. Available: http://ieeexplore.ieee.org/stamp/stamp.jsp?arnumber=5068387

[10] M. Kuhn, J. Turnmire, M. Mahfouz, and A. Fathy, "Adaptive leading-edge detection in UWB indoor localization," in *Radio and Wireless Symposium (RWS), 2010 IEEE*, 2010, pp. 268–271. [Online]. Available: http://ieeexplore.ieee.org/stamp/stamp.jsp?arnumber=5434259

[11] S. Marano, W. Gifford, H. Wymeersch, and M. Win, "NLOS identification and mitigation for localization based on UWB experimental data," *IEEE Journal on Selected Areas in Communications*, vol. 28, no. 7, pp. 1026–1035, 2010.

[12] M. Jing, Y. Z. Qin, and T. Z. Nai, "Impact of IR-UWB waveform distortion on NLOS localization system," in *Ultra-Wideband, 2009. ICUWB 2009. IEEE International Conference on*, 2009, pp. 123–128.

[13] P. Golik, P. Doetsch, and H. Ney, "Cross-entropy vs. squared error training: a theoretical and experimental comparison," in *Interspeech*, Lyon, France, Aug. 2013, pp. 1756–1760.